Neuromodulation of zebrafish primary motoneuron firing is shaped by developmental changes in the M-current

Stephanie F. Gaudreau[1] & Tuan V. Bui[1]

[1]Department of Biology, Brain and Mind Research Institute, University of Ottawa, Ontario, Canada, K1N 6N5

Correspondence: Tuan V. Bui (tuan.bui@uottawa.ca)

Running Title: Neuromodulation of the M-current in developing zebrafish motoneurons

Key points:

- The amplitude of the M-current is subject to modulation by several neuromodulators such as acetylcholine and serotonin
- Serotonin via $5HT_{1A}$ inhibits the M-current in primary motoneurons at 3 dpf
- Muscarinic agonist enhances the M-current in primary motoneurons after 3 dpf
- Neuromodulation of motoneuron firing properties by $5\text{-}HT_{1A}$ and muscarinic agonist is consistent with modulation of the M-current

Keywords: M-current, neuromodulation, primary motoneurons, zebrafish, serotonin, muscarine

ABSTRACT

Movements during development are refined through the ongoing maturation of the spinal circuits that mediate them. In many vertebrates, including zebrafish, this maturation process involves neuromodulators such as acetylcholine, serotonin, and dopamine; however, the targets of this neuromodulation remain largely unknown. Recent work has revealed distinct developmental dynamics of the non-inactivating subthreshold potassium current – the M-current – in primary motoneurons of larval zebrafish. Considering that neuromodulators play a role in the maturation of locomotor control in larval zebrafish, we asked whether neuromodulators might target the M-

current in primary motoneurons during development. Our patch-clamp experiments in primary motoneurons of zebrafish aged 3 to 5 days post-fertilization (dpf) reveal distinct modulation of the M-current by serotonin and acetylcholine that is age-dependent. Our data demonstrates an inhibitory influence of serotonin signaling via $5HT_{1A}$ receptors that promotes repetitive firing in primary motoneurons specifically at 3 dpf. We also show that acetylcholine, likely via M2/M4 receptors, enhances the M-current and limits repetitive firing in primary motoneurons but does so only after 3 dpf. Modulation of the M-current in primary motoneurons was not observed across all neuromodulators as dopamine had no effect at any age. Considering that the M-current transiently peaks at 3 dpf and is reduced at 4 and 5 dpf, our findings suggest that the developmental changes in this current can shape how neuromodulators modulate firing properties of primary motoneurons.

INTRODUCTION

Movement is generated by specialized neuronal networks located within the spinal cord. These spinal motor circuits must undergo progressive maturation during development to allow for increasingly refined and complex movements to be made. The exact changes spinal motor circuits undergo during maturation are not fully known but there is evidence supporting a role for neuromodulation in motor maturation. For example, both dopamine (DA) and serotonin (5-HT) have been shown to elicit air-stepping in spinally-transected neonatal rats, supporting their contributions to promoting hindlimb stepping (McEwen *et al.*, 1997). In the developing frog *Xenopus laevis,* 5-HT and noradrenaline have contrasting and coordinated influences on separate spinal locomotor circuits (Rauscent *et al.*, 2009). While effects to motor output by neuromodulatory systems during development have been described, little is known about the targets of this neuromodulation and the mechanisms by which they shape motor maturation.

The zebrafish is particularly well-suited for the study of motor maturation as their rapid development comprises stereotyped transitions in the movements they produce. Changes in motor behaviour can be readily linked to changes in underlying spinal circuitry. Indeed, DA and 5-HT have both been shown to have important influences on locomotor output during zebrafish development. DA signaling in the spinal cord mediates the important locomotor transition from 3 days post-fertilization (3 dpf) burst swimming to 4 dpf beat and glide swimming (Lambert *et al.*, 2012). It has also been shown to control the excitation of motoneurons (Jha & Thirumalai, 2020).

5-HT has been shown to limit the duration of periods of inactivity between successive swimming episodes in developing zebrafish (Brustein *et al.*, 2003). While these findings have proven important to our understanding of how supraspinal regions mediate flexible control over zebrafish spinal locomotor circuits in the context of development, the mechanisms by which these neuromodulators exert their influence on spinal neurons are unknown.

We have recently identified the presence of the non-inactivating subthreshold potassium current known as the M-current (I_M) in primary motoneurons (pMNs) of larval zebrafish. We show that I_M's influence on the control of excitability and regulation of repetitive firing changes during early zebrafish development, peaking at 3 dpf (Gaudreau & Bui, 2024). This coincides with the time when larvae are largely inactive and exhibit burst swimming, an immature form of swimming. By 4 dpf, their mature locomotor pattern – known as beat and glide swimming – emerges, and they swim much more frequently (Buss & Drapeau, 2001; Drapeau *et al.*, 2002).

Could I_M be a target for neuromodulation during development to facilitate motor maturation? As zebrafish transition from their embryonic stage characterized primarily of large amplitude and reflexive pMN-driven movements to their larval stage encompassing predominantly low amplitude secondary motoneuron (sMN) driven swimming, we posit that I_M in pMNs may be an important target for neuromodulation as pMN recruitment is restricted to specific movements (Liu & Westerfield, 1988; Menelaou & McLean, 2012; Wen *et al.*, 2020).

In this study, we use whole-cell electrophysiology to investigate how neuromodulators influence the properties of I_M in pMNs of larval zebrafish from 3 dpf to 5 dpf. Interestingly, we find that muscarine, a known inhibitor of I_M in other systems (Brown & Adams, 1980), does not inhibit I_M in pMNs of larval zebrafish and instead acts as an I_M enhancer. We find that enhancement of I_M by muscarine is age-dependent and coincides with ages where the current is relatively smaller. On the other hand, we observed inhibition of I_M by 5-HT via 5-HT_{1A} receptors. This inhibition is also age-dependent and occurs when I_M is at its largest within the developmental timeframe studied, namely at 3 dpf. Furthermore, we demonstrate that muscarine and a 5-HT_{1A} agonist modulate pMN firing in a manner consistent with their respective modulations of I_M.

METHODS

Animal Care

All experiments were performed in accordance with the protocol approved by the University of Ottawa's Animal Care Committee (BL-4416). As described previously (Gaudreau & Bui, 2025), adult zebrafish are maintained at 28.5°C with a 14 hour on/10 hour off light cycle, with lights off at 11PM and on at 9AM. Embryos are fertilized between 9AM-10AM and stored in embryo medium at 28.5°C until use for experimentation at 3 to 5 dpf.

Preparation for electrophysiology

Larval zebrafish were anesthetized in 0.02% tricaine (MS-222, Aqualife TMS; Syndel Laboratories) before being pinned down through the notochord onto a Sylgard (Dow Corning) coated dish using pins made of Tungsten wire (0.25 mm). Fish were spinalized at the level of segments 2-3 using fine surgical scissors, and the skin is then peeled back between the two pins using fine forceps. Next, muscles were dissociated by bathing larvae in 1 mg/mL collagenase (Millipore Sigma; incubation times: 10 minutes at 3 dpf, 12 minutes at 4 dpf, and 15 minutes at 5 dpf) to facilitate muscle removal. The collagenase solution is rinsed out 4-5 times with artificial cerebrospinal fluid (aCSF) containing: 134 mM NaCl, 2.9 mM KCl, 1.2 mM $MgCl_2$, 2.1 mM $CaCl_2$, 10 mM dextrose, and 10 mM HEPES (pH of 7.8 adjusted with NaOH and osmolarity between 280-290 adjusted with sucrose). Removal of muscles was done using suction through a wide-bored glass capillary whose tips were gently broken such that the tip was the appropriate size for muscle removal. To enable whole-cell patch-clamp electrophysiology, muscles overlaying the targeted spinal segments were removed.

Whole-cell patch-clamp electrophysiology

d-tubocurarine was added to the aCSF (10 μM; Millipore Sigma, catalog # 93750) to prevent muscle contractions. Electrodes for whole-cell patch-clamp experiments are made using borosilicate glass capillaries (Sutter Instrument; BF150-110-10) with typical tip resistances ranging from 5 to 7 MΩ. Intracellular recording solution used contained the following: 16 mM KCl, 116 mM K-gluconate, 4 mM $MgCl_2$, 10 mM HEPES, 10 mM EGTA, and 4 mM Na_2-ATP, adjusted to a pH of 7.2-7.3 with KOH. Osmolarity was adjusted to 270-280 mOsm with water. The initial descent of the electrode towards the spinal cord involved applying slight positive pressure.

Upon proximity to a pMN (targeted based on their distinctively large soma and mid-dorsoventral positioning), positive pressure was released to form a gigaohm (GΩ) seal. Pulses of negative pressure were used to break through the membrane. Membrane holding potential was quickly set to –65 mV and compensation of both fast and slow capacitance components was applied. Series resistance was routinely compensated for at 80% or higher. Values reported are not liquid junction potential corrected. Sulforhodamine B was added to the intracellular recording solution (0.1%; Millipore Sigma) to identify pMNs by visualization of their axon projection patterns. Electrical signals were amplified and filtered at 10 kHz or 20 kHz with a Multiclamp 700B (Axon Instruments, Molecular Devices),and digitized with a Digidata 1550 (Molecular Devices). A HumBug Noise Eliminator (Quest Scientific) attenuated 50/60 Hz electrical noise.

Voltage-clamp protocols and current estimations

I_M was revealed through the standard I_M deactivation protocol (Verneuil *et al.*, 2020; Sharples *et al.*, 2023) in voltage-clamp mode. The protocol consists of holding the neuron at -10 mV and introducing a series of hyperpolarizing voltage steps lasting 1 second each to deactivate I_M. The resulting loss of outward current caused by I_M deactivation can be used to estimate the amplitude of I_M. This calculation was made by taking the difference between the peak of the initial current response and the current at steady-state at the end of the step.

Current-clamp protocols and firing frequency measurements

500-ms current steps were applied to neurons initially held at -65 mV to calculate firing frequency. Rheobase was defined as the minimum current amplitude required to elicit an action potential. During a 500-ms current injection equal to 2x rheobase, the average instantaneous frequency of the last 5 pairs of action potentials was used to estimate steady-state firing frequency.

Pharmacology

Dopamine hydrochloride (3548, Tocris), serotonin hydrochloride (3547, Tocris), muscarine iodide (3074, Tocris), 5-HT_{1A} agonist 8-OH-DPAT (1080, Tocris), M2/M4 agonist oxotremorine-M (O100, Millipore Sigma), and 5-HT_{2A} agonist TCB-2 (2592, Tocris) were dissolved in water before final dissolution in aCSF of the recording bath. All drugs were introduced to the recording bath 5-10 minutes prior to recordings.

Data analysis and statistical analysis

We used the open-source pyABF python package in Spyder (version 5.1.5) to import and read electrophysiological data saved as .abf files. Python (version 3.9.12) scripts tailored to each type of recording enabled supervised, automated analysis of recordings. Prism by GraphPad (Version 10.5.0 (673) was used for statistical analyses and generation of graphs. The Shapiro-Wilk test was used to test all datasets for normality. For all tests, significance stars are displayed on graphs.

RESULTS

Muscarine enhances I_M in pMNs at 4 and 5 dpf

The discovery of I_M and its appellation originated from its inhibition by muscarine (Brown & Adams, 1980). Since our previous work identified I_M in pMNs of larval zebrafish (Gaudreau & Bui, 2024), we sought to investigate the potential for muscarinic inhibition of I_M in these neurons (**Fig. 1**). As described previously (Verneuil *et al.*, 2020; Sharples *et al.*, 2023; Gaudreau & Bui, 2024), we utilized the standard I_M voltage-clamp deactivation protocol to reveal its electrophysiological signature in current responses. Comparison of effects were made between three entirely distinct sample groups of pMNs: control pMNs and two groups of pMNs having been exposed to either 10 µM muscarine or 100 µM muscarine for several minutes prior to all recordings. Because of differences observed in the magnitude of I_M in pMNs during early zebrafish development, we compared the effects of muscarine at 3, 4, and 5 dpf. It is important to note that all data obtained from the control groups of pMNs presented here has been presented in prior work (Gaudreau & Bui, 2024). At 3 dpf, exposure to 10 µM muscarine and 100 µM muscarine did not alter the current-voltage relationship of I_M relative to control (**Fig. 1*A-B***). No significant differences in peak amplitude of I_M (control: 42.88 ± 18.44 pA; 10 µM muscarine: 50.56 ± 21.87 pA; 100 µM muscarine: 29.96 ± 18.99 pA; **Fig. 1*C***), I_M activation voltage (control: -54.55 ± 5.68 mV; 10 µM muscarine: -58.00 ± 9.19 mV; 100 µM muscarine: -49.00 ± 10.22 mV; **Fig. 1*D***), or the voltage at which I_M reaches half its maximal amplitude ($V_{1/2}$) (control: -47.64 ± 4.31 mV; 10 µM muscarine: -51.52 ± 6.99 mV; 100 µM muscarine: -43.98 ± 8.95 mV; **Fig. 1*E***) were observed between either 10 µM or 100 µM muscarine and controls. At 4 dpf, while 100 µM muscarine did not alter any of the properties of I_M, 10 µM muscarine enhanced I_M (**Fig. 1*F-J*)**. The average amplitude of I_M across voltages was significantly increased in pMNs exposed to 10 µM muscarine compared to controls (**Fig. 1*F-G***). The peak amplitude of I_M was also significantly increased in

pMNs exposed to 10 μM muscarine compared to control pMNs (control: 24.08 ± 10.91 pA; 10 μM muscarine: 42.86 ± 22.62 pA; 100 μM muscarine: 26.95 ± 15.81 pA; **Fig. 1*H***). The activation voltage of I_M (control: -45.63 ± 10.63 mV; 10 μM muscarine: -56.50 ± 3.38 mV; 100 μM muscarine: -49.09 ± 12.61 mV; **Fig. 1*I***) and $V_{1/2}$ (control: -41.90 ± 6.74 mV; 10 μM muscarine: -50.71 ± 4.30 mV; 100 μM muscarine: -42.06 ± 12.81 mV; **Fig. 1*J***) in pMNs were significantly hyperpolarized by 10 μM muscarine but remained unaltered by 100 μM muscarine compared to controls at 4 dpf. By 5 dpf, the average amplitude of I_M across voltages remains increased in pMNs exposed to 10 μM muscarine relative to control pMNs (**Fig. 1*K-L***) yet the peak amplitude is not significantly different between these groups (control: 28.63 ±11.56 pA; 10 μM muscarine: 39.59 ± 14.75 pA**; Fig. 1*M***). The current-voltage relationship of pMNs exposed to 100 μM muscarine compared to controls remained unchanged (**Fig. 1*K***) as did the peak amplitude of I_M (100 μM muscarine: 24.90 ± 10.53 pA; **Fig. 1*M***). The activation voltage of I_M was hyperpolarized by 10 μM but not 100 μM muscarine (control: -49.09 ± 7.06 mV; 10 μM muscarine: -56.36 ± 3.93 mV; 100 μM muscarine: -50.45 ± 6.11 mV; **Fig. 1*N***). Finally, the $V_{1/2}$ of I_M in pMNs exposed to either 10 or 100 μM muscarine was unchanged relative to controls (control: -47.79 ± 3.37 mV; 10 μM muscarine: -49.91 ± 2.94 mV; 100 μM muscarine: -41.43 ± 9.71 mV; **Fig. 1*O***). Overall, these data suggest that muscarine enhances I_M at a concentration of 10 μM, but not 100 μM, at 4 dpf and 5 dpf, but not 3 dpf.

Acetylcholine signaling via M2 & M4 receptors enhances I_M in pMNs at 4 dpf

Having revealed that muscarine enhances I_M in pMNs at 4 and 5 dpf, we wanted to identify the receptors via which acetylcholine (ACh) is exerting its influence. We bath applied 20 μM oxotremorine-M (Oxo-M), a broad muscarinic agonist with some reports of higher affinity for M2 and M4 receptors (Bevan, 1984; Caulfield & Brown, 1991), to pMNs and observed how the properties of I_M changed relative to control pMNs at 4 dpf. Oxo-M enhanced the average amplitude of I_M across voltages (**Fig. 2*A-B***) as well as the peak amplitude of I_M (control: 24.08 ± 10.91 pA; Oxo-M: 65.84 ± 18.92 pA; **Fig. 2*C***). Neither the activation voltage (control: -45.63 ± 10.63 mV; Oxo-M: -51.67 ± 4.33 mV; **Fig. 2*D***) nor $V_{1/2}$ (control: -41.90 ± 6.75 mV; Oxo-M: -46.43 ± 3.91 mV; **Fig. 2*E***) of I_M was altered in pMNs at 4 dpf. Overall, these results demonstrate that ACh signaling via M2/M4 receptors enhances I_M in pMNs at 4 dpf.

By 4 dpf, pMNs are able to repetitively fire during sustained depolarization (Gaudreau & Bui, 2024). We therefore investigated whether enhancing I_M in pMNs with Oxo-M reduced repetitive firing in pMNs at 4 dpf, To do this, we injected current equal to 2x rheobase into 4 dpf pMNs exposed to 20 µM Oxo-M compared their features of repetitive firing to control 4 dpf pMNs (**Fig. 2*F*-*G***). The number of action potentials produced significantly decreased in the presence of Oxo-M relative to control pMNs (control: 32.46 ± 23.85 spikes; Oxo-M: 7.33 ± 3.50 spikes; **Fig. 2*H***) while both steady-state firing frequency (control: 70.73 ± 36.11 Hz; Oxo-M: 95.45 ± 49.66 Hz; **Fig. 2*I***) and maximum instantaneous firing frequency remained unaffected (control: 360.00 ± 95.19 Hz; Oxo-M: 336.00 ±117.50 Hz; **Fig. 2*J***). Overall, these data suggest that the enhancing influence of M2/M4 signaling on I_M amplitude decreases the ability of pMNs to repetitively fire.

Dopamine does not alter the properties of I_M in pMNs of developing zebrafish

With the finding that muscarine does not inhibit I_M, unlike what has been shown in other species, we sought to determine whether the action of another neurotransmitter had inhibitory influences on I_M. Dopamine (DA) has been identified as a neuromodulator with important influence on the function of spinal locomotor circuits in zebrafish during development (Lambert *et al.*, 2012). We aimed to determine whether some of these previously reported effects of DA could be occurring via modulation of I_M by DA. To this end, we examined possible effects to the properties of I_M in pMNs exposed to either 10 µM or 100 µM DA at 3, 4, and 5 dpf. At 3 dpf, pMNs exposed to either 10 or 100 µM DA exhibited no changes to the current-voltage relationship of I_M (**Fig. 3*A*-*B***), the peak amplitude of I_M (control: 42.88 ± 18.44 pA; 10 µM dopamine: 44.97 ± 22.80 pA; 100 µM dopamine: 29.94 ± 10.44 pA; **Fig. 3*C***), its activation voltage (control: -54.55 ± 5.68 mV**;** 10 µM DA: -57.00 ± 4.22 mV; 100 µM DA: -55.45 ± 7.57 mV; **Fig. 3*D***), nor its $V_{1/2}$ (control: -47.64 ± 4.31 mV; 10 µM DA: -47.96 ± 6.44 mV; 100 µM DA: -46.04 ± 8.04 mV; **Fig. 3*E***) relative to controls. At 4 dpf, no significant effects by either 10 µM DA or 100 µM DA to the current-voltage relationship of I_M (**Fig. 3*F*-*G***), the peak amplitude of I_M (control: 24.08 ± 10.91 pA; 10 µM DA**:** 34.25 ± 16.81 pA; 100 µM DA: 22.96 ± 8.82 pA; **Fig. 3*H***), the activation voltage of I_M (control: -45.63 ± 10.63 mV; 10 µM DA: -53.33 ± 9.35 mV; 100 µM DA: -51.36 ± 6.74 mV; **Fig. 3*I***), or its $V_{1/2}$ (control: -41.90 ± 6.75 mV; 10 µM DA: -46.41 ± 7.62 mV; 100 µM DA: -44.44 ± 9.61 mV; **Fig. 3*J***) compared to control pMNs. Similarly, by 5 dpf, neither 10 µM DA nor 100 µM DA altered

the current-voltage relationship of I_M (**Fig. 3*K-L***), the peak amplitude of I_M (control: 28.63 ± 11.56 pA; 10 μM dopamine: 39.24 ± 9.96 pA; 100 μM dopamine: 23.50 ± 9.62 pA; **Fig. 2*M***), the activation voltage of I_M (control: -49.09 ± 7.01 mV; 10 μM dopamine: -53.89 ± 5.47 mV; 100 μM dopamine: -50.00 ± 7.07 mV; **Fig. 3*N***) nor its $V_{1/2}$ (control: -42.88 ± 9.03 mV; 10 μM dopamine: -44.73 ± 8.20 mV; 100 μM dopamine: -47.79 ± 3.37 mV; **Fig. 3*O***). Overall, these data reveal no effects of dopamine, at both concentrations tested, to the properties of I_M in 3 to 5 dpf pMNs.

Serotonin enhances I_M in pMNs at 4 dpf

Serotonin (5-HT) has been shown to inhibit I_M in pyramidal neurons of the weakly electric fish (Deemyad *et al.*, 2011) as well as neurons of the hypothalamus in mice (Roepke *et al.*, 2012). We therefore decided to test whether exogenous application of 5-HT at 20 μM and 100 μM altered properties of I_M in pMNs of larval zebrafish (**Fig. 4**). At 3 dpf, no differences between the current-voltage relationship of I_M (**Fig. 4*A-B***), the peak amplitude of I_M (control: 42.88 ± 18.44 pA ; 20 μM 5-HT: 47.95 ± 22.16 pA; 100 μM 5-HT: 35.07 ± 13.97 pA; **Fig. 4*C***), the activation voltage of I_M (control: -54.55 ± 5.68 mV; 20 μM 5-HT: -57.50 ± 5.40 mV; 100 μM 5-HT: -55.00 ± 7.50 mV; **Fig. 4*D***) or its $V_{1/2}$ (control: -37.64 ± 4.31 mV; 20 μM 5-HT: -51.76 ± 3.59 mV; 100 μM 5-HT: -47.92 ± 5.12 mV; **Fig. 4*E***) in pMNs across treatment groups were observed. By 4 dpf, the average amplitude of I_M across voltages is increased in pMNs by 20 μM 5-HT, but not 100 μM 5-HT, compared to controls (**Fig. 4*F-G***). Similarly, 20 μM 5-HT, but not 100 μM 5-HT, increases the peak amplitude of I_M measured in pMNs compared to controls (control: 24.08 ± 10.91 pA; 20 μM 5-HT: 42.36 ± 15.31 pA; 100 μM 5-HT: 27.94 ± 15.59 pA; **Fig. 4*H***). The activation voltage of I_M remains unchanged by 20 μM 5-HT and 100 μM 5-HT compared to controls (control: -45.63 ± 10.63 mV; 20 μM 5-HT: -51.67 ± 6.85 mV; 100 μM 5-HT: -45.42 ± 9.16 mV; **Fig. 4*I***). Neither 20 μM or 100 μM 5-HT altered $V_{1/2}$ relative to controls (control: -41.90 ± 6.75 mV; 20 μM 5-HT: -46.51 ± 6.07 mV; 100 μM 5-HT: -39.83 ± 8.21 mV; **Fig. 4*J***). By 5 dpf, there are no differences across treatment groups to the current-voltage relationship of I_M (**Fig. 4*K-L***), the peak amplitude of I_M (control: 28.63 ± 11.56 pA; 20 μM 5-HT: 34.95 ± 15.17 pA; 100 μM 5-HT: 37.53 ± 22.82 pA; **Fig. 4*M***), the activation voltage of I_M (control: -49.09 ± 7.01 mV; 20 μM 5-HT: -51.54 ± 8.26 mV; 100 μM 5-HT: -47.50 ± 3.78 mV; nor I_M's $V_{1/2}$ (control: -47.79 ± 3.37 mV; 20 μM 5-HT: -45.35 ± 7.02 mV; 100 μM 5-HT: -43.06 ± 3.25 mV; **Fig. 4*O***). These findings reveal that 5-HT at 20 μM may have an overall enhancing effect on I_M that is most prominent at 4 dpf.

Serotonin does not modulate I_M in pMNs via $5HT_{2A}$ receptors

We next furthered our investigation into the role of serotonin in the modulation of I_M in pMNs of developing zebrafish by investigating how the selective $5HT_{2A}$ receptor agonist TCB-2 influences properties of I_M. As with the experiments described above, we compared the properties of I_M between two distinct groups of pMNs, one being control pMNs and the other being pMNs exposed to 10 μM TCB-2 before recordings began. At 3 dpf, TCB-2 does not alter the current-voltage relationship of I_M (**Fig. 5*A-B***), its peak amplitude (control: 42.88 ± 18.44 pA; TCB-2: 40.86 ± 17.38 pA; **Fig. 5*C***), activation voltage (control: -54.55 ± 5.68 mV; TCB-2: -55.55 ± 7.70 mV; **Fig. 5*D***), or its $V_{1/2}$ (control: -49.39 ± 6.19 mV; TCB-2: -47.64 ± 4.31 mV; **Fig. 5*E***). This is also the case at 4 dpf, where TCB-2 does not significantly influence the current-voltage relationship of I_M (**Fig. 5*F-G***), its peak amplitude (control: 24.08 ± 10.91 pA; TCB-2: 25.15 ± 9.31 pA; **Fig. 5*H***), activation voltage (control: -45.63 ± 10.63 mV; TCB-2: -45.45 ± 7.23 mV; **Fig. 5*I***), or $V_{1/2}$ (control: -41.90 ± 6.75 mV; TCB-2: -43.34 ± 6.04 mV; **Fig. 5*J***). Similarly, by 5 dpf, the current-voltage relationship (**Fig. 5*K-L***), peak amplitude (control: 28.63 ± 11.56 pA; TCB-2: 29.26 ± 9.67 pA; **Fig. 5*M***), activation voltage (control: -49.09 ± 7.01 mV; TCB-2: -49.09 ± 7.36 mV; **Fig. 5*N***), and $V_{1/2}$ (control: -47.79 ± 3.37 mV; TCB-2: -44.45 ± 7.06 mV; **Fig. 5*O***) of I_M are not altered by TCB-2 relative to controls. These results demonstrate that serotonin via $5HT_{2A}$ receptors does not modulate I_M in pMNs from 3 to 5 dpf.

Serotonin via $5HT_{1A}$ receptors inhibits I_M in pMNs at 3 dpf

Since our TCB-2 experiments revealed no modulation of I_M in pMNs by serotonin via $5HT_{2A}$ receptors, we next investigated serotonin's possible influence on I_M via $5HT_{1A}$ receptors. We compared the properties of I_M in pMNs exposed to 10 μM 8-OH-DPAT to those of control pMNs at 3, 4, and 5 dpf. At 3 dpf, we find that 8-OH-DPAT inhibits I_M as is observed by a significant decrease in the average amplitude of I_M across voltages (**Fig. 6*A-B***) and the peak amplitude of I_M (control: 42.88 ± 18.44 pA; 10 μM 8-OH-DPAT: 22.94 ± 11.05 pA; **Fig. 6*C***). I_M's activation voltage (control: -54.44 ± 5.68 mV; 10 μM 8-OH-DPAT: -52.50 ± 10.34 mV; **Fig. 6*D***) and $V_{1/2}$ (control: -47.64 ± 4.31 mV; 10 μM 8-OH-DPAT: -42.29 ± 7.37 mV; **Fig. 6*E***) remained unchanged by 8-OH-DPAT in pMNs at 3 dpf. At 4 dpf, 8-OH-DPAT does not alter the current-voltage relationship of I_M (**Fig. 6*F-G***), the peak amplitude of I_M (control: 24.08 ± 10.91 pA; 10 μM 8-OH-

DPAT: 31.62 ± 26.83 pA; **Fig. 6*H***), the activation voltage of I_M (control: -45.63 ± 10.63 mV; 10 μM 8-OH-DPAT: -50.91 ± 9.44 mV; **Fig. 6*I***), nor I_M's $V_{1/2}$ (control: -41.90 ± 6.75 mV**;** 10 μM 8-OH-DPAT: -45.42 ± 10.78 mV; **Fig. 6*J***) in pMNs compared to controls. Similarly, at 5 dpf, 8-OH-DPAT does not alter the current-voltage relationship of I_M (**Fig. 6*K-L***), the peak amplitude of I_M (control: 28.63 ± 11.56 pA; 10 μM 8-OH-DPAT: 34.14 ± 15.99 pA; **Fig. 6*M***), nor I_M's $V_{1/2}$ (control: -47.79 ± 3.37 mV; 10 μM 8-OH-DPAT: -49.87 ± 3.66 mV; **Fig. 6*O***) in pMNs compared to controls. TCB-2 does however hyperpolarize the activation voltage of I_M (control: -49.09 ± 7.01 mV; 10 μM 8-OH-DPAT: -55.56 ± 4.64 mV; **Fig. 6*N***). These data support an inhibitory influence of serotonin signaling via 5-HT_{1A} receptors on I_M specifically at 3 dpf.

Serotonin signaling via $5HT_{1A}$ receptors increases repetitive firing in pMNs at 3 dpf

We have previously shown that inhibiting I_M with 10 μM XE-991 in pMNs increased their ability to repetitively fire at 3 dpf, the age at which I_M appears to be largest in magnitude during early development (Gaudreau & Bui, 2024). Having identified $5HT_{1A}$ receptors as mediating serotonin's inhibitory influence over I_M, we aimed to investigate whether 8-OH-DPAT increased the ability of 3 dpf pMNs to repetitively fire in a manner similar to application of the I_M-specific inhibitor XE-991. To do this, we injected 3 dpf pMNs exposed to 10 μM 8-OH-DPAT with current equal to 2x rheobase and compared their features of repetitive firing to control 3 dpf pMNs (**Fig. 7*A-B***). We find that 8-OH-DPAT significantly increases the number of spikes generated (control: 8.33 ± 6.85 spikes; 8-OH-DPAT: 23.00 ± 13.38 spikes; **Fig. 7*C***) as well as the steady-state firing frequency (control: 29.73 ± 3.71 Hz; 8-OH-DPAT: 58.36 ± 22.83 Hz; **Fig. 7*D***) while the maximum instantaneous firing frequency remained unchanged (control: 392.2 ± 185.0 Hz; 8-OH-DPAT: 337.3 ± 94.2 Hz; **Fig. 7*E***) relative to control pMNs. Overall, these results suggest that serotonin via $5HT_{1A}$ receptors can promote repetitive firing in pMNs via inhibition of I_M at 3 dpf.

DISCUSSION

Neuromodulators such as DA and 5-HT are known to influence motor maturation, as evidenced by work in the developing zebrafish (Brustein *et al.*, 2003; Lambert *et al.*, 2012). Specific neuronal targets of this modulation however remain largely unknown as do the mechanism by which neuromodulators exert their influence on neurons. In this study, we investigated the subthreshold non-inactivating potassium current, I_M, as a possible target for neuromodulation in spinal locomotor circuits of the developing zebrafish. I_M shows non-monotonic developmental dynamics in pMNs during a time period where zebrafish transition from crude, ballistic coiling movements to more refined swimming maneuvers characterized by low-amplitude repetitive tail beats (Gaudreau & Bui, 2024). At the same time, the firing properties of pMNs mature with decreasing spike frequency adaptation and increased sustained firing (Gaudreau & Bui, 2024). We reasoned that neuromodulation of I_M may also shift during this time period of rapid changes in the amplitude of this current. We characterized the influence of muscarine, DA, and 5-HT on the activity of I_M in primary motoneurons from 3 to 5 dpf as developing zebrafish undergo motor maturation (summarized in **Fig. 8**).

Muscarine as an I_M enhancer in pMNs of developing zebrafish

I_M was designated as the M-current based on the finding that it was inhibited by muscarine at the time of its discovery (Brown & Adams, 1980). Because of this, we had expected to see inhibition of I_M in pMNs exposed to muscarine. Intriguingly however, we found that muscarine instead had an enhancing effect on I_M in pMNs at 4 and 5 dpf with no effects observed at 3 dpf. Traditional inhibition of I_M by muscarine is mediated by muscarinic acetylcholine receptors (mAChRs) coupled to $G_{q/11}$ proteins whose activation leads to the eventual depletion of phosphatidylinositol 4,5-biphosphate (PIP_2) at the membrane which directly influences the activity of Kv7.2/7.3 channels that mediate I_M (Zhang *et al.*, 2003; Suh & Hille, 2007). A study in neurons of the mouse dentate gyrus however reveals that, contrary to most other findings, acetylcholine signaling via M_1 receptors actually enhances the activity of I_M by increasing levels of PIP_2 (Carver & Shapiro, 2019). In line with these findings, our data support the idea that cholinergic influence over levels of PIP_2 through muscarinic receptors, and subsequently I_M activity is neuron-specific and can deviate from the usual suppression of this current. We demonstrate that the preferential M2/M4 mAChR agonist oxotremorine-M enhances I_M in 4 dpf pMNs, raising the possibility that in these

neurons M2 or M4 mAChR activation may ultimately lead to increased PIP_2 levels. Alternatively, this enhancement of I_M could be brought on by a PIP_2-independent mechanism (Marrion, 1997). Regardless of the precise mAChRs and mechanisms involved, our data reveals functional impact of I_M enhancement by M2/M4 activation wherein oxotremorine-M limits the ability of pMNs to repetitively fire. Activation of M2 mAChRs in fast motoneurons of the adult zebrafish also limits their spiking activity (Bertuzzi & Ampatzis, 2018). Our data raises the possibility that I_M in fast motoneurons could continue to be the target of cholinergic influence on decreased repetitive firing in the adult zebrafish. Further studies are necessary to uncover both the source of acetylcholine – cholinergic spinal V2a (Guan *et al.*, 2021) and V0c neurons being prime candidates (Kelly *et al.*, 2023) – and the contexts in which mAChRs might be activated to enhance I_M, and consequently limit firing, in pMNs.

Serotonin as both an enhancer and inhibitor of I_M in pMNs of developing zebrafish

Exogenous application of 5-HT leads to obvious enhancing of I_M in pMNs at 4 dpf, but not at 3 or 5 dpf. When we specifically target 5-HT_{1A} receptors using the selective agonist 8-OH-DPAT, however, we find that I_M is inhibited in pMNs at 3 dpf. Several instances of opposing roles of 5-HT on the excitability of individual neurons have been observed in other systems. For example, 5-HT_2 receptor mediated serotonergic signaling caused membrane depolarization while 5-HT_{1A} receptor mediated serotonergic signaling resulted in hyperpolarization in pyramidal cells of the cortex in rats (Araneda & Andrade, 1991). In turtle motoneurons, application of 5-HT to the dendritic tree promoted plateau potentials through 5-HT_{2A} activation whereas application to the perisomatic region sometimes inhibited spike generation through 5-$HT_{1A/7}$ receptors (Perrier & Hounsgaard, 2003; Perrier & Cotel, 2008). This raises the intriguing possibility that the lack of effect of 5-HT on I_M in 3 dpf pMN despite the inhibition observed by activation of 5-HT_{1A} receptors through 8-OH-DPAT administration is due to the presence of a different 5-HT receptor subtype that increases I_M at that age, and that these two receptors are distributed at different locations. Electrophysiology experiments testing the effects of additional 5-HT receptor subtypes, other than $5HT_{1A}$ and $5HT_{2A}$, on the properties of I_M in pMNs would reveal which receptor is responsible for the 5-HT-driven enhancement of I_M that we have observed, further delineating the mechanisms underlying I_M modulation.

Concentration-dependent neuromodulation of spinal locomotor networks

The presence of multiple receptor subtypes on a single neuron can help explain concentration-dependent effects that we observed. In our investigation into the effects of muscarine, DA, and 5-HT, on the modulation of I_M, we bath-applied each neuromodulator at relatively low and high concentrations. 5-HT and muscarine both changed the magnitude of I_M at the lower concentrations – 20 and 10 μM, respectively – while showing no effects at 100 μM relative to controls. With distinct receptors having varying affinities for their respective neuromodulators, the ultimate effect to I_M in pMNs is likely to depend both on the identity of receptors expressed and the concentration of neuromodulator present. Indeed, modulatory action of DA on the activity of rat hypothalamus neurons is concentration-dependent, with low versus high levels of DA determining the direction of dopaminergic modulation (Linehan *et al.*, 2015). Opposing effects of DA in the striatum (Stoof & Kebabian, 1981) has long been shown to affect motor control (Kravitz *et al.*, 2010). This type of dual complimentary action of neuromodulators has also been observed within spinal locomotor networks across species. ACh, DA, and 5-HT can each exert opposing or concentration-dependent influences on motor output that is dependent on the receptor subtypes activated within each neuromodulator system (Harris-Warrick & Cohen, 1985; Clemens *et al.*, 2012; Sharples *et al.*, 2015; Nascimento *et al.*, 2019). At the motoneuron level, it has been demonstrated in the adult zebrafish that M2 activation decreases firing while activation of other mAChRs increases firing (Bertuzzi & Ampatzis, 2018). We therefore posit that the observed lack of effect of higher doses of serotonin and muscarine can be attributed to the broad activation of receptor subtypes that may ultimately mask effects brought on by activation of higher affinity receptors at lower neuromodulator concentrations. Identification and precise pharmacological targeting of specific neuromodulator receptor subtypes expressed in pMNs is necessary to delineate concentration-dependent effects of neuromodulators to the magnitude of I_M in these neurons.

Developmental changes to neuromodulatory influence on I_M in pMNs of developing zebrafish

In addition to having uncovered neuromodulators that differentially modulate the activity of I_M, we have revealed age-related differences in the effects of these neuromodulators during the 3 to 5 dpf time window. We show that muscarine enhances I_M at 4 and 5 dpf, but not at 3 dpf. This is particularly intriguing as this coincides with the reduction in the magnitude of I_M we have observed

from 3 dpf to 4 and 5 dpf. It appears as though when I_M is already prominent in pMNs at 3 dpf, there is no mAChR-mediated enhancement of I_M. Furthermore, we show that 5-HT_{1A} receptor agonist 8-OH-DPAT inhibits I_M, but only at 3 dpf when the magnitude of I_M in pMNs is largest during the investigated time period. In this case, it appears that when basal levels of I_M are low, as they are at 4 and 5 dpf, there is no 5-HT_{1A} mediated inhibition of I_M. These findings support the idea that different neuromodulator systems work together to fine-tune basal activity levels of I_M that change during development. At 3 dpf when larvae are largely inactive, I_M in pMNs is large. Inhibition of I_M by 5-HT_{1A} signaling may help recruit pMNs for fast movements by alleviating the control I_M has on pMN excitability and repetitive firing. Acetylcholine via mAChRs may only come into play as an enhancer of I_M by 4-5 dpf because there may be no need for further enhancement of I_M at 3 dpf. By 4-5 dpf when larvae are more active, I_M is reduced in magnitude in pMNs compared to 3 dpf. At this point, pMNs may benefit from I_M enhancement by ACh in contexts where pMN excitability and/or repetitive firing should be limited, for example during transitions from fast to slow swims when pMNs are no longer needed. Whether the push-pull effects that serotonin and acetylcholine exert on I_M at different ages, which seems to depend on when the amplitude of this current is high or low, relies on the same biochemical pathway (e.g. PIP_2 signaling) or separate pathways, remains to be determined.

Behavioural contexts of I_M neuromodulation in pMNs

We have shown that I_M in pMNs is a target of neuromodulation by 5-HT and ACh. Putatively through enhancement and inhibition of I_M, 5-HT and ACh increases and limits, respectively, the ability of pMNs to repetitively fire. This raises the question: in what contexts would I_M in pMNs need to be modulated? pMNs are recruited primarily during fast and crude movements such as coilings, escapes, fast swims, and struggling (Liu & Westerfield, 1988; Liao & Fetcho, 2008; McLean & Fetcho, 2009; Tong & McDearmid, 2012; Wen *et al.*, 2020). Neuromodulation by DA has been shown to prime pMNs for involvement in optomotor responses through modulation of their intrinsic properties (Jha & Thirumalai, 2020). Therefore, neuromodulation of I_M could also help ensure the degree to which pMNs repetitively fire during various movements, as evidenced by the effect of pharmacological modulation of this current on escapes and swimming (Gaudreau & Bui, 2025). For example, ACh could enhance I_M to limit pMN firing during the fastest swims requiring high-frequency tail beats while 5-HT could inhibit I_M to promote repetitive firing in the

case of struggling when long-lasting muscle contraction is required (Liao & Fetcho, 2008). Neuromodulation of I_M in pMNs may supplement circuit connectivity to ensure smooth transitions between swim speeds and appropriate muscle contraction for effective struggling. Indeed, neuromodulation may be more powerful than synaptic inputs in influencing motoneuron excitability and overall motor output (Heckman *et al.*, 2009).

To conclude, we have revealed how different neuromodulators influence pMN firing through I_M. We identify two neuromodulator systems that serve as a means to regulate the activity of pMNs in opposite directions via modulation of I_M and also reveal how their respective influences on I_M varies within a short developmental time window depending on the age-dependent fluctuations of this current. This work highlights how distinct neuromodulators can exert complimentary and dynamic influences on the activity of ion currents during development, perhaps to facilitate changes to spinal locomotor circuits during motor maturation.

DATA AVAILABILITY

Data will be made available upon request.

ACKNOWLEDGMENTS

We would like to thank John Lewis, Michael Jonz, Emily Standen, and Minoru Koyama for their valuable input during the study. This work was supported by the Natural Sciences and Engineering Research Council of Canada (NSERC): NSERC Discovery Grant, Grant Number: RGPIN-2022-03898 (to TVB); NSERC Canadian Graduate Scholarship M award, Award Number: NSERC 553401-2020 (to SFG); NSERC Postgraduate Scholarship D, Award Number: 569969-2022 (to SFG).

AUTHOR CONTRIBUTIONS

SFG: Conceived and designed research, performed experiments, analyzed data, interpreted results of experiments, prepared figures, drafted manuscript, edited and revised manuscript.

TVB: Conceived and designed research, drafted manuscript, edited and revised manuscript, and approved final version of the manuscript.

DISCLOSURES

The authors declare no competing interests.

REFERENCES

Araneda R & Andrade R (1991). 5-Hydroxytryptamine2 and 5-hydroxytryptamine1A receptors mediate opposing responses on membrane excitability in rat association cortex. *Neuroscience* **40,** 399–412.

Bertuzzi M & Ampatzis K (2018). Spinal cholinergic interneurons differentially control motoneuron excitability and alter the locomotor network operational range. *Sci Rep* **8,** 1988.

Bevan P (1984). [3H]Oxotremorine-M binding to membranes prepared from rat brain and heart: Evidence for subtypes of muscarinic receptors. *European Journal of Pharmacology* **101,** 101–110.

Brown DA & Adams PR (1980). Muscarinic suppression of a novel voltage-sensitive K+ current in a vertebrate neurone. *Nature* **283,** 673–676.

Brustein E, Chong M, Holmqvist B & Drapeau P (2003). Serotonin patterns locomotor network activity in the developing zebrafish by modulating quiescent periods. *J Neurobiol* **57,** 303–322.

Buss RR & Drapeau P (2001). Synaptic Drive to Motoneurons During Fictive Swimming in the Developing Zebrafish. *Journal of Neurophysiology* **86,** 197–210.

Carver CM & Shapiro MS (2019). Gq-Coupled Muscarinic Receptor Enhancement of KCNQ2/3 Channels and Activation of TRPC Channels in Multimodal Control of Excitability in Dentate Gyrus Granule Cells. *J Neurosci* **39,** 1566–1587.

Caulfield MP & Brown DA (1991). Pharmacology of the putative M4 muscarinic receptor mediating Ca-current inhibition in neuroblastoma x glioma hybrid (NG 108-15) cells. *Br J Pharmacol* **104,** 39–44.

Clemens S, Belin-Rauscent A, Simmers J & Combes D (2012). Opposing modulatory effects of D1- and D2-like receptor activation on a spinal central pattern generator. *Journal of Neurophysiology* **107,** 2250–2259.

Deemyad T, Maler L & Chacron MJ (2011). Inhibition of SK and M channel-mediated currents by 5-HT enables parallel processing by bursts and isolated spikes. *J Neurophysiol* **105,** 1276–1294.

Drapeau P, Saint-Amant L, Buss RR, Chong M, McDearmid JR & Brustein E (2002). Development of the locomotor network in zebrafish. *Progress in Neurobiology* **68,** 85–111.

Gaudreau SF & Bui TV (2024). Developmental changes in the control of primary motoneuron excitability by the M-current in larval zebrafish. 2024.10.17.618843. Available at: https://www.biorxiv.org/content/10.1101/2024.10.17.618843v1 [Accessed September 7, 2025].

Gaudreau SF & Bui TV (2025). Pharmacological modulation of the M-current shapes locomotor function in developing zebrafish. *Journal of Neurophysiology*; DOI: 10.1152/jn.00003.2025.

Guan NN, Xu L, Zhang T, Huang C-X, Wang Z, Dahlberg E, Wang H, Wang F, Pallucchi I, Hua Y, El Manira A & Song J (2021). A specialized spinal circuit for command amplification and directionality during escape behavior. *Proceedings of the National Academy of Sciences* **118,** e2106785118.

Harris-Warrick RM & Cohen AH (1985). Serotonin Modulates the Central Pattern Generator for Locomotion in the Isolated Lamprey Spinal Cord. *J Exp Biol* **116,** 27–46.

Heckman CJ, Mottram C, Quinlan K, Theiss R & Schuster J (2009). Motoneuron excitability: the importance of neuromodulatory inputs. *Clin Neurophysiol* **120,** 2040–2054.

Jha U & Thirumalai V (2020). Neuromodulatory selection of motor neuron recruitment patterns in a visuomotor behavior increases speed. *Curr Biol* **30,** 788-801.e3.

Kelly JJ, Wen H & Brehm P (2023). Single-cell RNAseq analysis of spinal locomotor circuitry in larval zebrafish ed. Beam K & Huguenard JR. *eLife* **12,** RP89338.

Kravitz AV, Freeze BS, Parker PRL, Kay K, Thwin MT, Deisseroth K & Kreitzer AC (2010). Regulation of parkinsonian motor behaviours by optogenetic control of basal ganglia circuitry. *Nature* **466,** 622–626.

Lambert AM, Bonkowsky JL & Masino MA (2012). The Conserved Dopaminergic Diencephalospinal Tract Mediates Vertebrate Locomotor Development in Zebrafish Larvae. *J Neurosci* **32,** 13488–13500.

Liao JC & Fetcho JR (2008). Shared versus Specialized Glycinergic Spinal Interneurons in Axial Motor Circuits of Larval Zebrafish. *J Neurosci* **28,** 12982–12992.

Linehan V, Trask RB, Briggs C, Rowe TM & Hirasawa M (2015). Concentration-dependent activation of dopamine receptors differentially modulates GABA release onto orexin neurons. *Eur J Neurosci* **42,** 1976–1983.

Liu DW & Westerfield M (1988). Function of identified motoneurones and co-ordination of primary and secondary motor systems during zebra fish swimming. *J Physiol* **403,** 73–89.

Marrion NV (1997). Control of M-current. *Annu Rev Physiol* **59,** 483–504.

McEwen ML, Van Hartesveldt C & Stehouwer DJ (1997). L-DOPA and quipazine elicit air-stepping in neonatal rats with spinal cord transections. *Behavioral Neuroscience* **111,** 825–833.

McLean DL & Fetcho JR (2009). Spinal Interneurons Differentiate Sequentially from Those Driving the Fastest Swimming Movements in Larval Zebrafish to Those Driving the Slowest Ones. *J Neurosci* **29,** 13566–13577.

Menelaou E & McLean DL (2012). A Gradient in Endogenous Rhythmicity and Oscillatory Drive Matches Recruitment Order in an Axial Motor Pool. *Journal of Neuroscience* **32,** 10925–10939.

Nascimento F, Spindler LRB & Miles GB (2019). Balanced cholinergic modulation of spinal locomotor circuits via M2 and M3 muscarinic receptors. *Sci Rep* **9,** 14051.

Perrier J-F & Cotel F (2008). Serotonin differentially modulates the intrinsic properties of spinal motoneurons from the adult turtle. *J Physiol* **586,** 1233–1238.

Perrier J-F & Hounsgaard J (2003). 5-HT2 Receptors Promote Plateau Potentials in Turtle Spinal Motoneurons by Facilitating an L-Type Calcium Current. *Journal of Neurophysiology* **89,** 954–959.

Rauscent A, Einum J, Le Ray D, Simmers J & Combes D (2009). Opposing aminergic modulation of distinct spinal locomotor circuits and their functional coupling during amphibian metamorphosis. *J Neurosci* **29,** 1163–1174.

Roepke TA, Smith AW, Rønnekleiv OK & Kelly MJ (2012). Serotonin 5-HT2C receptor-mediated inhibition of the M-current in hypothalamic POMC neurons. *Am J Physiol Endocrinol Metab* **302,** E1399-1406.

Sharples SA, Broadhead MJ, Gray JA & Miles GB (2023). M-type potassium currents differentially affect activation of motoneuron subtypes and tune recruitment gain. *The Journal of Physiology* **601,** 5751–5775.

Sharples SA, Humphreys JM, Jensen AM, Dhoopar S, Delaloye N, Clemens S & Whelan PJ (2015). Dopaminergic modulation of locomotor network activity in the neonatal mouse spinal cord. *Journal of Neurophysiology* **113,** 2500–2510.

Stoof JC & Kebabian JW (1981). Opposing roles for D-1 and D-2 dopamine receptors in efflux of cyclic AMP from rat neostriatum. *Nature* **294,** 366–368.

Suh B-C & Hille B (2007). Regulation of KCNQ channels by manipulation of phosphoinositides. *J Physiol* **582,** 911–916.

Tong H & McDearmid JR (2012). Pacemaker and plateau potentials shape output of a developing locomotor network. *Current Biology* **22,** 2285–2293.

Verneuil J, Brocard C, Trouplin V, Villard L, Peyronnet-Roux J & Brocard F (2020). The M-current works in tandem with the persistent sodium current to set the speed of locomotion. *PLOS Biology* **18,** e3000738.

Wen H, Eckenstein K, Weihrauch V, Stigloher C & Brehm P (2020). Primary and secondary motoneurons use different calcium channel types to control escape and swimming behaviors in zebrafish. *Proc Natl Acad Sci U S A* **117,** 26429–26437.

Zhang H, Craciun LC, Mirshahi T, Rohács T, Lopes CMB, Jin T & Logothetis DE (2003). PIP2 Activates KCNQ Channels, and Its Hydrolysis Underlies Receptor-Mediated Inhibition of M Currents. *Neuron* **37,** 963–975.

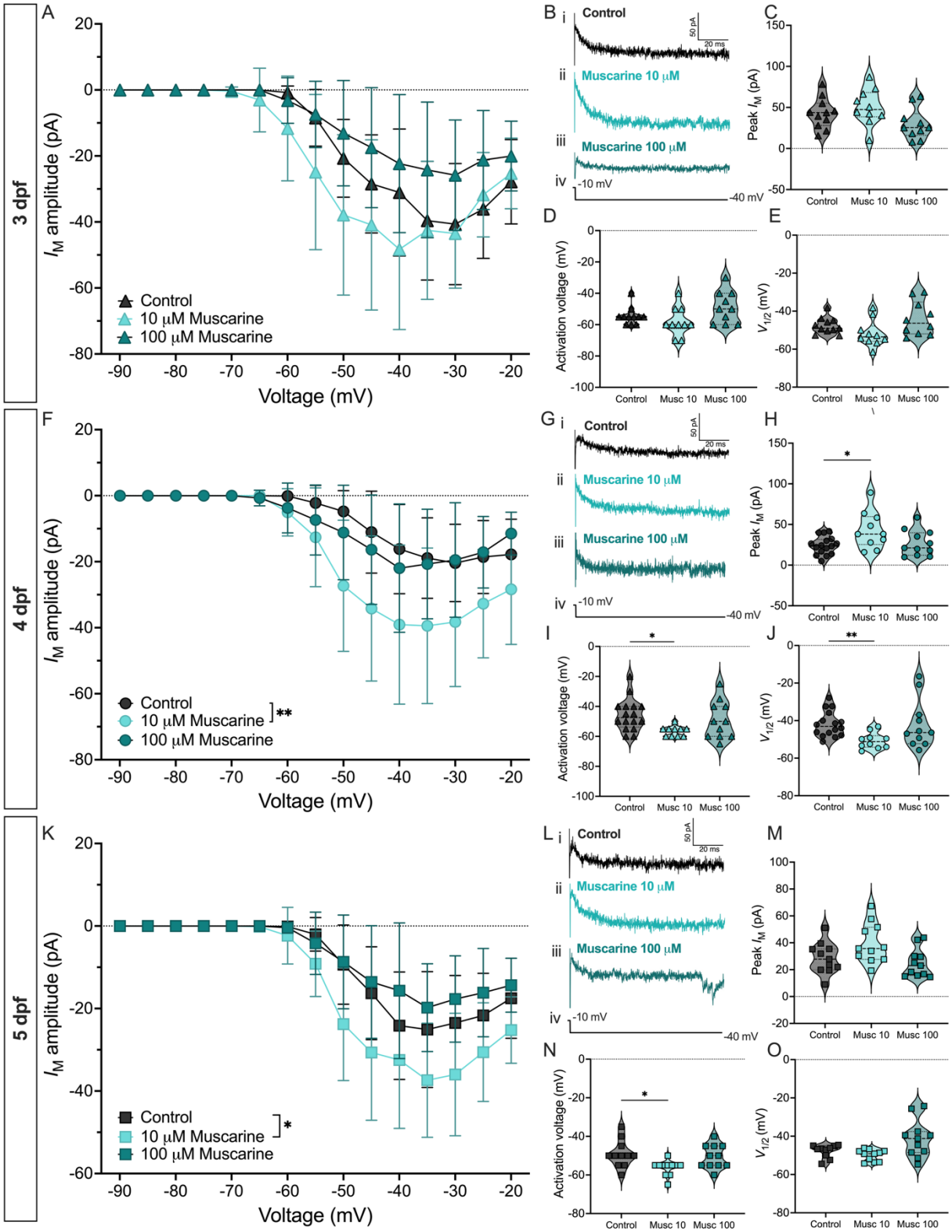
3 dpf
4 dpf
5 dpf
A
F
K
I_M amplitude (pA)
Voltage (mV)
Control
10 μM Muscarine
100 μM Muscarine
**
*
B
G
L
i
ii
iii
iv
Control
Muscarine 10 μM
Muscarine 100 μM
50 pA
20 ms
-10 mV
-40 mV
C
H
M
Peak I_M (pA)
D
I
N
Activation voltage (mV)
E
J
O
$V_{1/2}$ (mV)
Control
Musc 10
Musc 100

Figure 1. Muscarine enhances I_M in pMNs of developing zebrafish after 3 dpf. ***A***, Current-voltage relationship of I_M in three groups of 3 dpf pMNs: control (n = 11, N = 6), 10 μM muscarine (Musc 10; n = 10, N = 4), 100 μM muscarine (Musc 100; n = 10, N = 4). ***B***, Examples of current responses from (*i*) control, (*ii*) 10 μM muscarine, and (*iii*) 100 μM muscarine pMNs in response to (*iv*) a -30 mV hyperpolarizing voltage step at 3 dpf. ***C***, Peak amplitude of I_M across treatment groups at 3 dpf. ***D***, Activation voltage of I_M across treatment groups at 3 dpf. ***E***, Voltage at which I_M reaches half its maximal amplitude ($V_{1/2}$) across treatment group at 3 dpf. ***F***, Current-voltage relationship of I_M in three groups of 4 dpf pMNs: control (n = 16, N = 6), 10 μM muscarine (n = 10, N = 3), 100 μM muscarine (n = 11, N = 5). ***G***, Examples of current responses from (*i*) control, (*ii*) 10 μM muscarine, and (*iii*) 100 μM muscarine pMNs in response to (*iv*) a -30 mV hyperpolarizing voltage step at 4 dpf. ***H***, Peak amplitude of I_M across the treatment groups at 4 dpf. ***I***, Activation voltage of I_M across treatment groups at 4 dpf. ***J***, Voltage at which I_M reaches half its maximal amplitude ($V_{1/2}$) across treatment group at 4 dpf. ***K***, Current-voltage relationship of I_M in three groups of 5 dpf pMNs: control (n = 11, N = 5), 10 μM muscarine (n = 11, N = 3), 100 μM muscarine (n = 11, N = 4). ***L***, Examples of current responses from (*i*) control, (*ii*) 10 μM muscarine, and (*iii*) 10 μM muscarine pMNs in response to (*iv*) a -30 mV hyperpolarizing voltage step at 5 dpf. ***M***, Peak amplitude of I_M across the treatment groups at 5 dpf. ***N***, Activation voltage of I_M across treatment groups at 5 dpf. ***O***, Voltage at which I_M reaches half its maximal amplitude ($V_{1/2}$) across treatment group at 5 dpf (control: n = 10, N = 5; rest of sample sizes same as in ***K***). *Statistical analysis,* (***A***, ***F***, ***K***) mixed-effects analysis, (***D***, ***I-J***, ***N-O***) Kruskal-Wallis test with Dunn's test for multiple comparisons, and (***C***, ***E***, ***H***, ***M***) ordinary one-way ANOVA with Dunnett's test for multiple comparisons: * $P < 0.05$, ** $P < 0.01$; otherwise, not statistically significant.

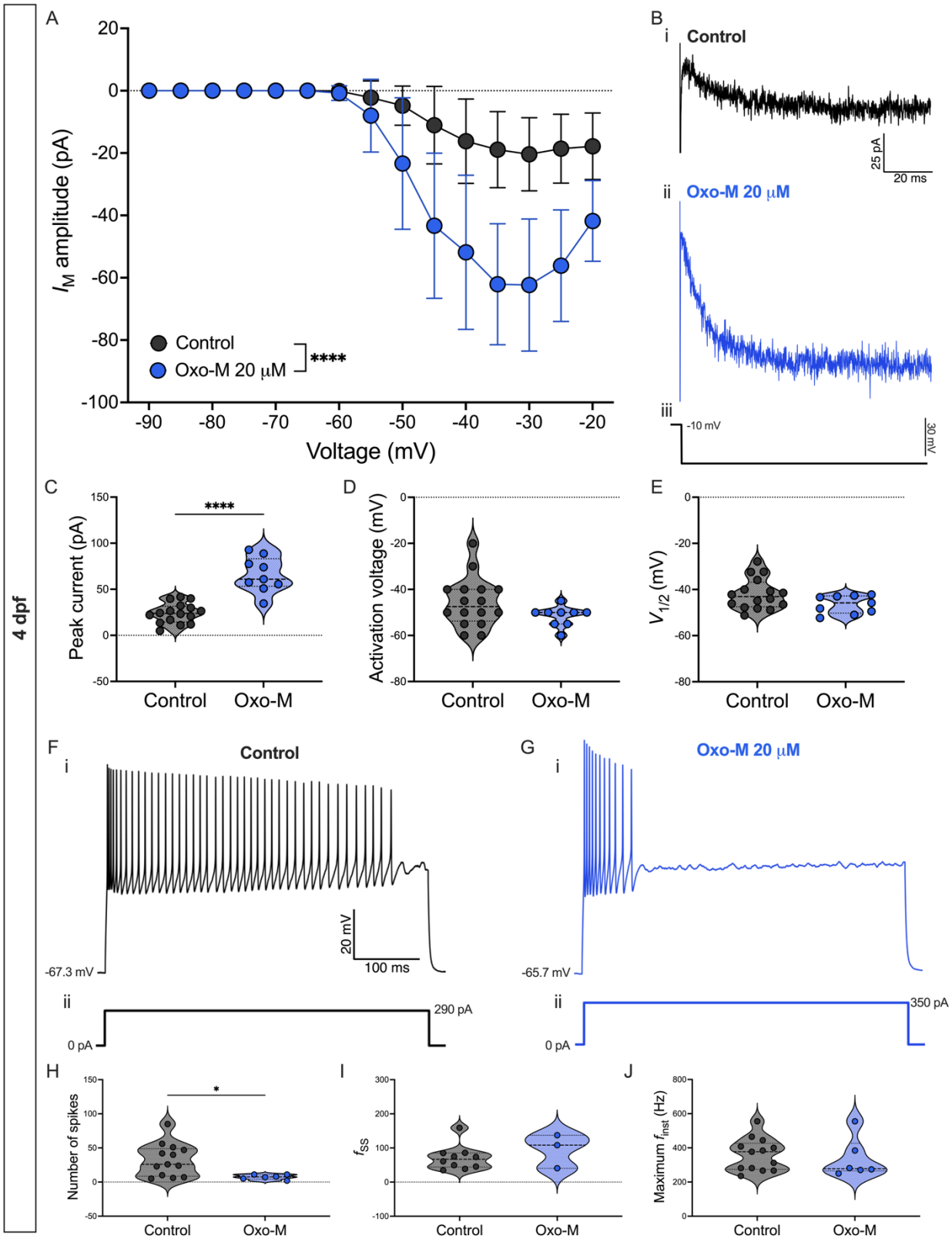
4 dpf
A
I_M amplitude (pA)
Voltage (mV)
Control
Oxo-M 20 μM
****
B
i Control
25 pA
20 ms
ii Oxo-M 20 μM
iii
-10 mV
30 mV
C
Peak current (pA)
****
Control
Oxo-M
D
Activation voltage (mV)
Control
Oxo-M
E
$V_{1/2}$ (mV)
Control
Oxo-M
F
i Control
20 mV
100 ms
-67.3 mV
ii
290 pA
0 pA
G
i Oxo-M 20 μM
-65.7 mV
ii
350 pA
0 pA
H
Number of spikes
*
Control
Oxo-M
I
f_{SS}
Control
Oxo-M
J
Maximum f_{inst} (Hz)
Control
Oxo-M

Figure 2. mAChR agonist enhances I_M in pMNs at 4 dpf. ***A***, Current-voltage relationship of I_M in control pMNs (black) and those exposed to 20 μM oxotremorine-M (Oxo-M) at 3 dpf. ***B***, Example current responses of (***i***) a control pMN (n = 16, N = 7) and (***ii***) a pMN exposed to 20 μM Oxo-M (n = 9; N = 4) in response to (***iii***) a negative 30 mV step from -10 mV holding during standard I_M deactivation protocol. ***C***, Peak I_M amplitude. ***D***, Activation voltage of I_M. ***E***, Voltage at which I_M reaches half its maximal amplitude ($V_{1/2}$). ***F-G***, Representative current-clamp responses of (***Fi***) control pMNs and ***Gi***) those exposed to 20 μM Oxo-M in response to (***ii***) a current injection equal to 2x rheobase. ***H***, Number of spikes generated in response to a 2x rheobase current injection (control: n = 13, N = 5; Oxo-M: n = 6, N = 5). ***I***, Steady-state instantaneous firing frequency calculated from responses to a 2x rheobase current injection (control: n = 10, N =5; Oxo-M: n = 3, N = 2). ***J***, Maximum instantaneous firing frequency reached during responses to a 2x rheobase current injection (sample sizes are the same as in ***H***). *Statistical analysis,* (***A***) mixed-effects analysis, (***C-E***, ***H***) unpaired t-test and (***I-J***) Mann-Whitney tests. * $P < 0.05$, **** $P < 0.0001$; otherwise, not statistically significant.

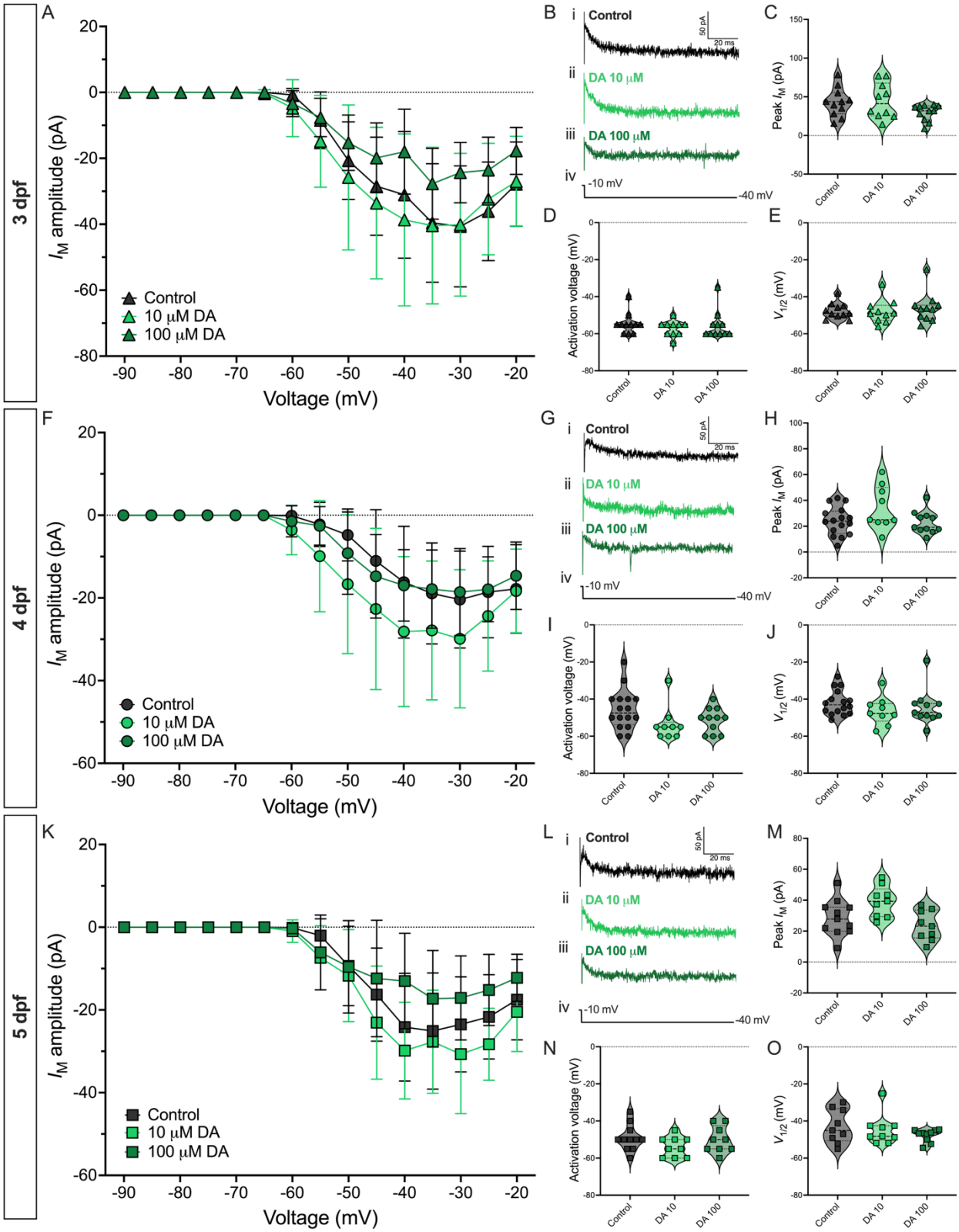
3 dpf
4 dpf
5 dpf
A
B
C
D
E
F
G
H
I
J
K
L
M
N
O
I_M amplitude (pA)
Voltage (mV)
Control
10 μM DA
100 μM DA
DA 10 μM
DA 100 μM
-10 mV
-40 mV
50 pA
20 ms
Peak I_M (pA)
Activation voltage (mV)
$V_{1/2}$ (mV)
DA 10
DA 100

Figure 3. Dopamine does not modulate I_M in pMNs of developing zebrafish. ***A***, Current-voltage relationship of I_M in three groups of 3 dpf pMNs: control (n = 11, N = 6), 10 μM dopamine (DA) (n = 10, N = 3), 100 μM dopamine (n = 11, N = 3). ***B***, Examples of current responses from (*i*) control, (*ii*) 10 μM dopamine, and (*iii*) 10 μM dopamine pMNs in response to (*iv*) a -30 mV hyperpolarizing voltage step at 3 dpf. ***C***, Peak amplitude of I_M across treatment groups at 3 dpf. ***D***, Activation voltage of I_M across treatment groups at 3 dpf. ***E***, Voltage at which I_M reaches half its maximal amplitude ($V_{1/2}$) across treatment group at 3 dpf. ***F***, Current-voltage relationship of I_M in three groups of 4 dpf pMNs: control (n = 16, N = 6), 10 μM dopamine (n = 9, N = 3), 100 μM dopamine (n = 11, N = 3). ***G***, Examples of current responses from (*i*) control, (*ii*) 10 μM dopamine, and (*iii*) 100 μM dopamine pMNs in response to (*iv*) a -30 mV hyperpolarizing voltage step at 4 dpf. ***H***, Peak amplitude of I_M across the treatment groups at 4 dpf. ***I***, Activation voltage of I_M across treatment groups at 4 dpf. ***J***, Voltage at which I_M reaches half its maximal amplitude ($V_{1/2}$) across treatment group at 4 dpf. ***K***, Current-voltage relationship of I_M in three groups of 5 dpf pMNs: control (n = 11, N = 5), 10 μM dopamine (n = 9, N = 5), 100 μM dopamine (n = 9, N = 3). ***L***, Examples of current responses from (*i*) control, (*ii*) 10 μM dopamine, and (*iii*) 100 μM dopamine pMNs in response to (*iv*) a -30 mV hyperpolarizing voltage step at 5 dpf. ***M***, Peak amplitude of I_M across the treatment groups at 5 dpf. ***N***, Activation voltage of I_M across treatment groups at 5 dpf. ***O***, Voltage at which I_M reaches half its maximal amplitude ($V_{1/2}$) across treatment group at 5 dpf. *Statistical analysis,* (***A***, ***F***, ***K***) mixed-effects analysis, (***D***-***E***, ***I***-***J***, ***M***, ***O***) Kruskal-Wallis test with Dunn's test for multiple comparisons, and (***C***, ***H***, ***N***) ordinary one-way ANOVA with Dunnett's test for multiple comparisons.

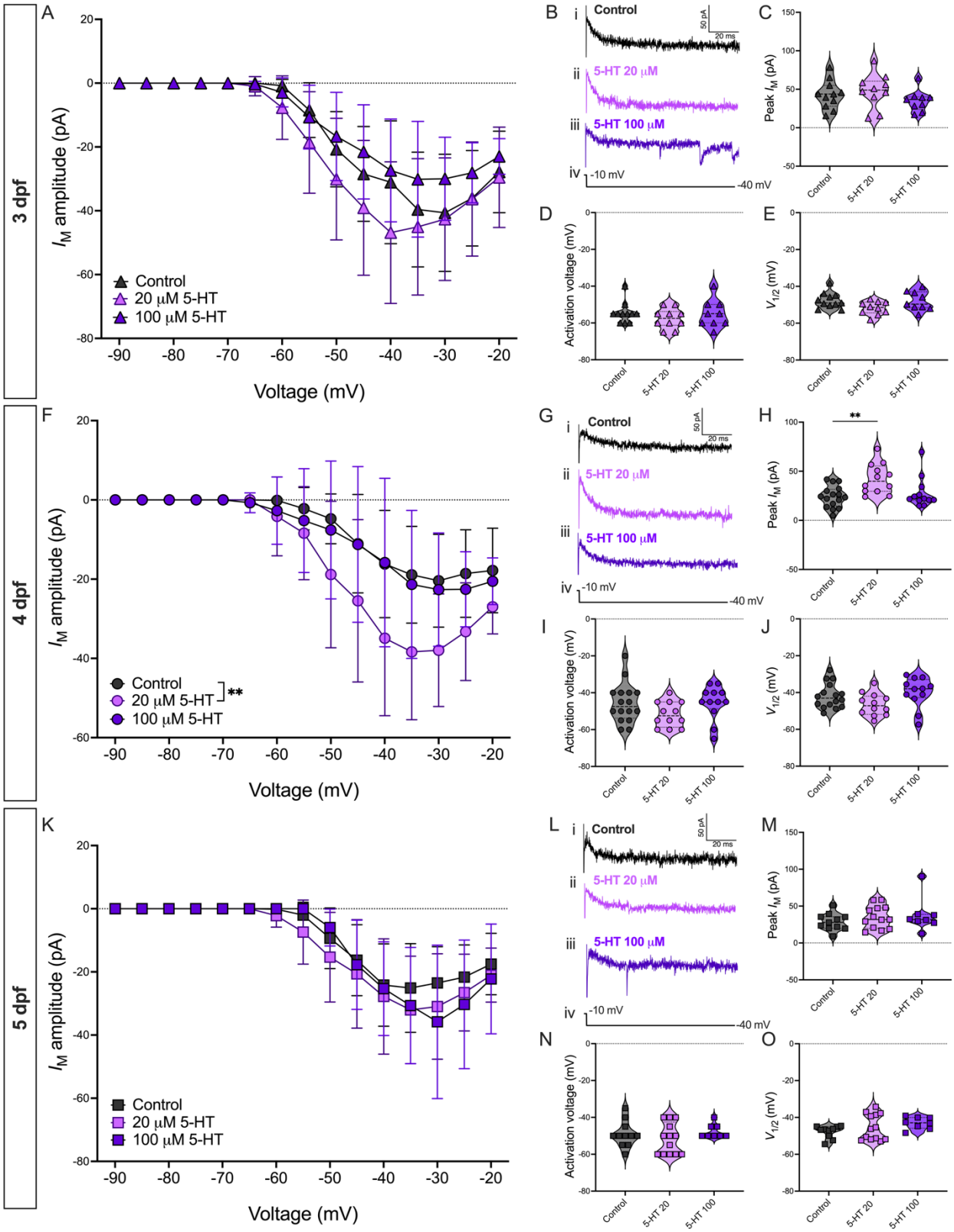
3 dpf
4 dpf
5 dpf
A
B
C
D
E
F
G
H
I
J
K
L
M
N
O
I_M amplitude (pA)
Voltage (mV)
Control
20 μM 5-HT
100 μM 5-HT
5-HT 20 μM
5-HT 100 μM
-10 mV
-40 mV
50 pA
20 ms
Peak I_M (pA)
Activation voltage (mV)
$V_{1/2}$ (mV)
5-HT 20
5-HT 100
**

Figure 4. Serotonin enhances I_M in pMNs of developing zebrafish at 4 dpf. ***A***, Current-voltage relationship of I_M in three groups of 3 dpf pMNs: control (n = 11, N = 6), 20 μM serotonin (5-HT) (n = 10, N = 5), 100 μM 5-HT (n = 9, N = 5). ***B***, Examples of current responses from (*i*) control, (*ii*) 20 μM 5-HT, and (*iii*) 100 μM 5-HT pMNs in response to (*iv*) a -30 mV hyperpolarizing voltage step at 3 dpf. ***C***, Peak amplitude of I_M across treatment groups at 3 dpf. ***D***, Activation voltage of I_M across treatment groups at 3 dpf. ***E***, Voltage at which I_M reaches half its maximal amplitude ($V_{1/2}$) across treatment group at 3 dpf. ***F***, Current-voltage relationship of I_M in three groups of 4 dpf pMNs: control (n = 16, N = 6), 20 μM 5-HT (n = 12, N = 4), 100 μM 5-HT (n = 12, N = 6). ***G***, Examples of current responses from (*i*) control, (*ii*) 20 μM 5-HT and (*iii*) 100 μM 5-HT pMNs in response to (*iv*) a -30 mV hyperpolarizing voltage step at 4 dpf. ***H***, Peak amplitude of I_M across the treatment groups at 4 dpf. ***I***, Activation voltage of I_M across treatment groups at 4 dpf. ***J***, Voltage at which I_M reaches half its maximal amplitude ($V_{1/2}$) across treatment group at 4 dpf. ***K***, Current-voltage relationship of I_M in three groups of 5 dpf pMNs: control (n = 11, N = 5), 20 μM 5-HT (n = 13, N = 5), 100 μM 5-HT (n = 8, N = 4). ***L***, Examples of current responses from (*i*) control, (*ii*) 20 μM 5-HT, and (*iii*) 100 μM 5-HT pMNs in response to (*iv*) a -30 mV hyperpolarizing voltage step at 5 dpf. ***M***, Peak amplitude of I_M across the treatment groups at 5 dpf. ***N***, Activation voltage of I_M across treatment groups at 5 dpf. ***O***, Voltage at which I_M reaches half its maximal amplitude ($V_{1/2}$) across treatment group at 5 dpf. *Statistical analysis,* (***A***, ***F***, ***K***) mixed-effects analysis, (***H***, ***M***-***O***) Kruskal-Wallis test with Dunn's test for multiple comparisons, and (***D***-***E***, ***I***-***J***) ordinary one-way ANOVA with Dunnett's test for multiple comparisons: ** P < 0.01; otherwise, not statistically significant.

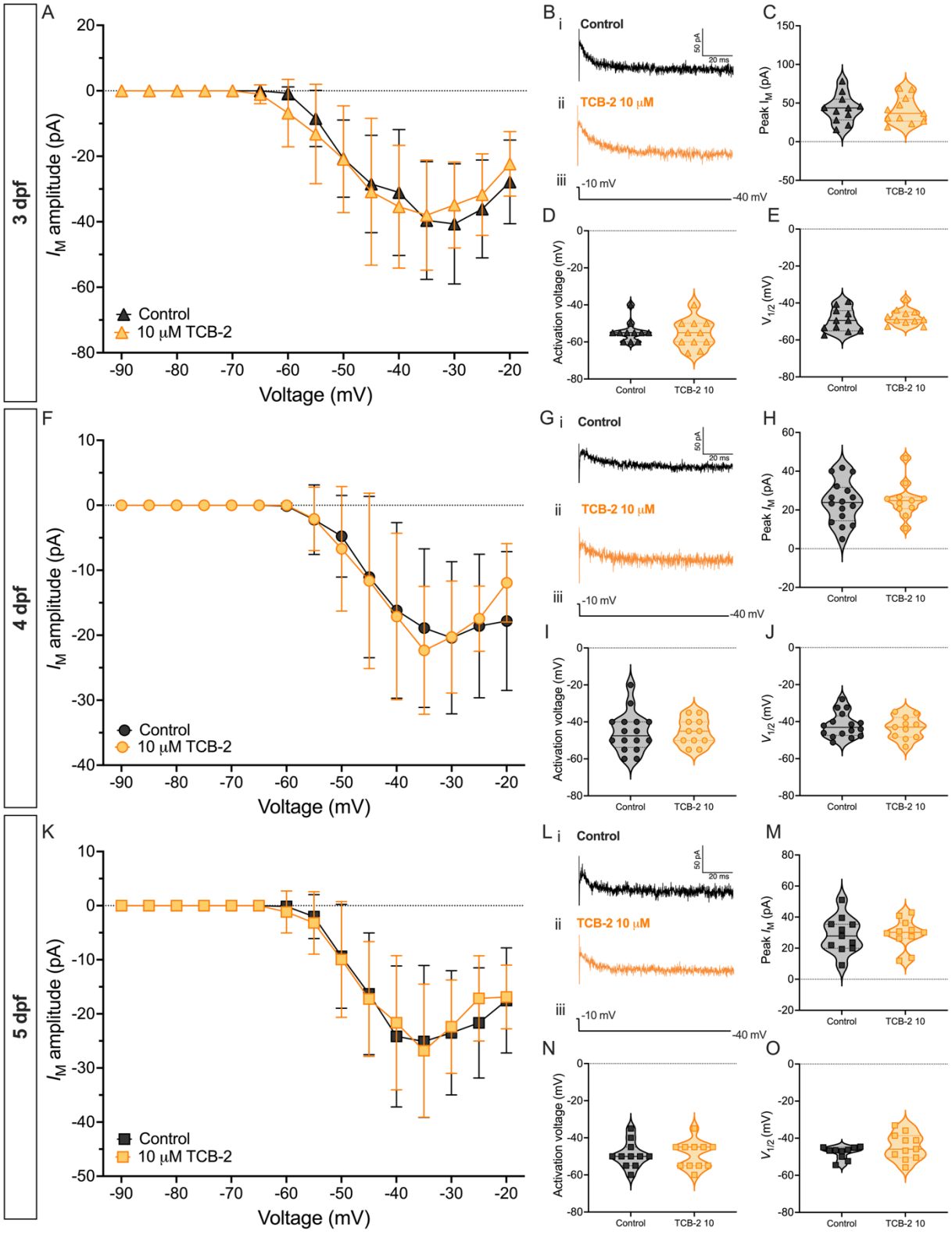
3 dpf
4 dpf
5 dpf
A
F
K
I_M amplitude (pA)
Voltage (mV)
Control
10 μM TCB-2
B
G
L
i Control
ii TCB-2 10 μM
iii -10 mV
-40 mV
50 pA
20 ms
C
H
M
Peak I_M (pA)
D
I
N
Activation voltage (mV)
E
J
O
$V_{1/2}$ (mV)
Control
TCB-2 10

Figure 5. 5HT$_{2A}$ agonist does not modulate I_M in pMNs during zebrafish development. ***A***, Current-voltage relationship of I_M in two groups of 3 dpf pMNs: control (n = 11, N = 6) and 10 µM TCB-2 (n = 11, N = 5). ***B***, Examples of current responses from (*i*) control and (*ii*) 10 µM TCB-2 pMNs in response to (*iii*) a -30 mV hyperpolarizing voltage step at 3 dpf. ***C***, Peak amplitude of I_M across treatment groups at 3 dpf. ***D***, Activation voltage of I_M across treatment groups at 3 dpf. ***E***, Voltage at which I_M reaches half its maximal amplitude ($V_{1/2}$) across treatment group at 3 dpf. ***F***, Current-voltage relationship of I_M in two groups of 4 dpf pMNs: control (n = 16, N = 6), and 10 µM TCB-2 (n = 11, N = 4). ***G***, Examples of current responses from (*i*) control and (*ii*) 10 µM TCB-2 pMNs in response to (*iii*) a -30 mV hyperpolarizing voltage step at 4 dpf. ***H***, Peak amplitude of I_M across the treatment groups at 4 dpf. ***I***, Activation voltage of I_M across treatment groups at 4 dpf. ***J***, Voltage at which I_M reaches half its maximal amplitude ($V_{1/2}$) across treatment group at 4 dpf. ***K***, Current-voltage relationship of I_M in two groups of 5 dpf pMNs: control (n = 11, N = 5) and 10 µM TCB-2 (n = 11, N = 5). ***L***, Examples of current responses from (*i*) control and (*ii*) 10 µM TCB-2 pMNs in response to (*iii*) a -30 mV hyperpolarizing voltage step at 5 dpf. ***M***, Peak amplitude of I_M across the treatment groups at 5 dpf. ***N***, Activation voltage of I_M across treatment groups at 5 dpf. ***O***, Voltage at which I_M reaches half its maximal amplitude ($V_{1/2}$) across treatment group at 5 dpf. *Statistical analysis,* (***A***, ***F***, ***K***) mixed-effects analysis, (***C***, ***H-J***, ***M-N***) unpaired t-tests, and (***D***, ***O***) Mann-Whitney tests.

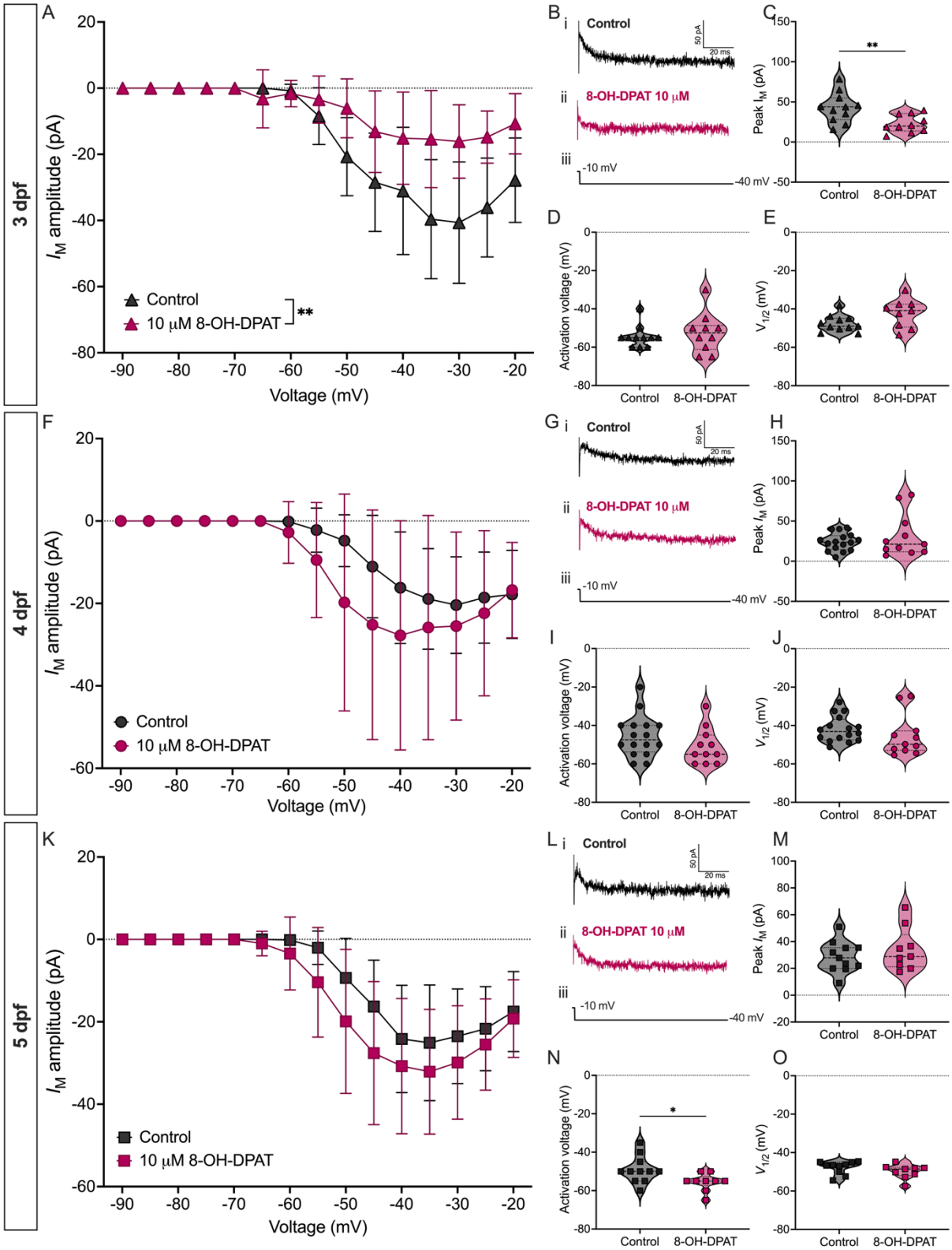
3 dpf
4 dpf
5 dpf
A
B
C
D
E
F
G
H
I
J
K
L
M
N
O
I_M amplitude (pA)
Voltage (mV)
Control
10 μM 8-OH-DPAT
**
8-OH-DPAT 10 μM
50 pA
20 ms
-10 mV
-40 mV
Peak I_M (pA)
Activation voltage (mV)
$V_{1/2}$ (mV)
*

Figure 6. $5HT_{1A}$ agonist inhibits I_M in pMNs at 3 dpf. ***A***, Current-voltage relationship of I_M in two groups of 3 dpf pMNs: control (n = 11, N = 6) and 10 μM 8-OH-DPAT (n = 10, N = 4). ***B***, Examples of current responses from (*i*) control and (*ii*) 10 μM 8-OH-DPAT pMNs in response to (*iii*) a -30 mV hyperpolarizing voltage step at 3 dpf. ***C***, Peak amplitude of I_M across treatment groups at 3 dpf. ***D***, Activation voltage of I_M across treatment groups at 3 dpf. ***E***, Voltage at which I_M reaches half its maximal amplitude ($V_{1/2}$) across treatment group at 3 dpf. ***F***, Current-voltage relationship of I_M in two groups of 4 dpf pMNs: control (n = 16, N = 6), and 10 μM 8-OH-DPAT (n = 11, N = 5). ***G***, Examples of current responses from (*i*) control and (*ii*) 10 μM 8-OH-DPAT pMNs in response to (*iii*) a -30 mV hyperpolarizing voltage step at 4 dpf. ***H***, Peak amplitude of I_M across the treatment groups at 4 dpf. ***I***, Activation voltage of I_M across treatment groups at 4 dpf. ***J***, Voltage at which I_M reaches half its maximal amplitude ($V_{1/2}$) across treatment group at 4 dpf. ***K***, Current-voltage relationship of I_M in two groups of 5 dpf pMNs: control (n = 11, N = 5) and 10 μM 8-OH-DPAT (n = 9, N = 4). ***L***, Examples of current responses from (*i*) control and (*ii*) 10 μM 8-OH-DPAT pMNs in response to (*iii*) a -30 mV hyperpolarizing voltage step at 5 dpf. ***M***, Peak amplitude of I_M across the treatment groups at 5 dpf. ***N***, Activation voltage of I_M across treatment groups at 5 dpf. ***O***, Voltage at which I_M reaches half its maximal amplitude ($V_{1/2}$) across treatment group at 5 dpf. *Statistical analysis,* (***A***, ***F***, ***K***) mixed-effects analysis, (***C***, ***E***, ***I***, ***M***-***N***) unpaired t-tests, and (***D***, ***H***, ***J***, ***O***) Mann-Whitney tests: * $P < 0.05$, ** $P < 0.01$; otherwise, not statistically significant.

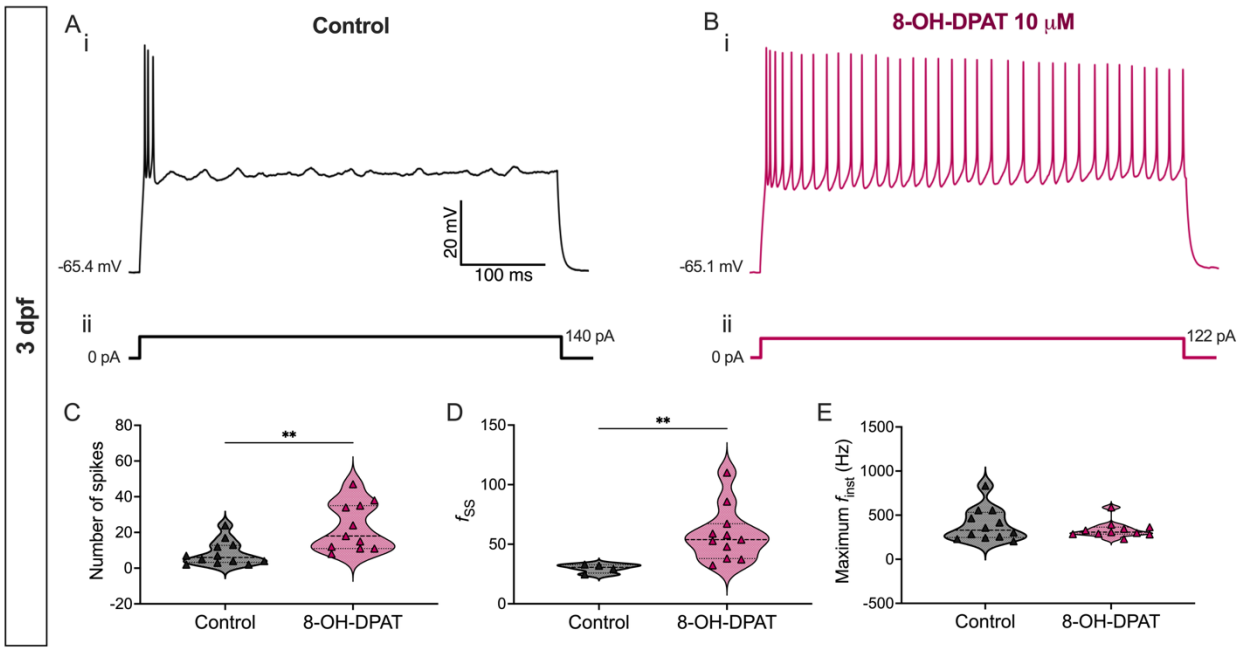

Figure 7. 5-HT$_{1A}$ agonist increases repetitive firing in pMNs at 3 dpf. ***A-B***, Representative current-clamp responses of (***Ai***) control pMNs and (***Bi***) those exposed to 10 μM 8-OH-DPAT in response to (***ii***) a current injection equal to 2x rheobase. ***C***, Number of spikes generated in response to a 2x rheobase current injection (control: $n = 12$, $N = 6$; 8-OH-DPAT: $n = 11$, $N = 5$). ***D***, Steady-state instantaneous firing frequency calculated from responses to a 2x rheobase current injection (sample sizes are the same as in ***C***). ***E***, Maximum instantaneous firing frequency reached during responses to a 2x rheobase current injection (control: $n = 4$, $N = 2$; 8-OH-DPAT: $n = 11$, $N = 5$). *Statistical analysis,* Mann-Whitney tests. ** $P < 0.01$; otherwise, not statistically significant.

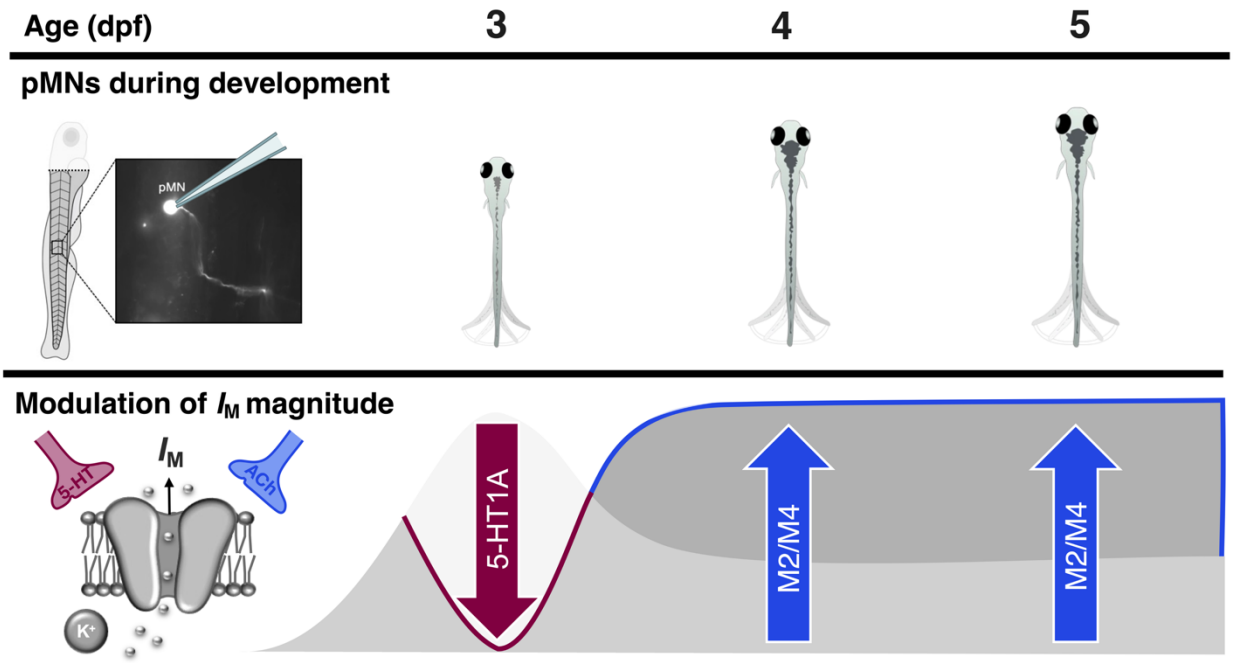

Figure 8. Distinct modulatory influence of serotonin and acetylcholine on I_M in pMNs during zebrafish development. At 3 dpf, when the magnitude of I_M peaks (Gaudreau & Bui, 2024) during early zebrafish development, serotonin signaling via $5HT_{1A}$ receptors acts to inhibit I_M. By 3 dpf, when the magnitude of I_M has subsequently decreased, equivalent activation of $5HT_{1A}$ receptors no longer inhibits I_M. Instead, we find that at this age, I_M is subject to enhancement by acetylcholine via M2/M4 receptors. I_M in pMNs may present itself as a dial for neuromodulation to fine-tune pMN excitability and firing activity during zebrafish development.